DOI: 10.1002/ejic.200900302

A New Trigonal-Bipyramidal $[Cu^{II}(pytBuN_3)Cl_2]$ Complex: Synthesis, Structure and Ligand Substitution Behaviour

Shaban Y. Shaban,[a] Frank W. Heinemann,[a] and Rudi van Eldik*[a]

Keywords: Copper / Chelates / Copper(II) complexes / Kinetics / UV/Vis spectroscopy / Biphasic reaction

The synthesis, structure and ligand substitution mechanism of a new five-coordinate copper(II) complex with a sterically constrained py*t*BuN$_3$ chelate ligand [py*t*BuN$_3$ = 2,6-bis(3,5-di-*tert*-butylphenyliminomethyl)pyridine] are reported. In the crystal structure of the complex the [Cu(py*t*BuN$_3$)Cl$_2$] chromophore possesses a distorted trigonal-bipyramidal coordination geometry. The kinetics and mechanism of chloride substitution by thiourea (TU) and *N*,*N*,*N*′,*N*′-tetramethylthiourea (TMTU) were studied in detail as a function of nucleophile concentration, temperature and pressure in methanol as solvent. The kinetics showed that the substitution reaction of [Cu(py*t*BuN$_3$)Cl$_2$] is a biphasic process that involves the subsequent displacement of both chloride ligands. The substitution of the first chloride by TU, $k_1^{296} = 918 \pm 30$ M^{-1}s^{-1}, is 570 times faster than the substitution of the second chloride, $k_2^{296} = 1.62 \pm 0.06$ M^{-1}s^{-1}. Substitution of chloride by TU is characterized by the activation parameters: $\Delta H^{\#} = 42 \pm 2$ and 58 ± 2 kJ mol^{-1}, $\Delta S^{\#} = -46 \pm 7$ and -47 ± 6 J K^{-1} mol^{-1}, and $\Delta V^{\#} = -6.5 \pm 0.2$ and -5.3 ± 0.7 cm^3 mol^{-1}, for the first and second substitution reactions, respectively. It is concluded from the activation parameters that both reactions follow an associative interchange (I$_a$) mechanism. When the substitution reaction was carried out with the sterically hindered nucleophile TMTU, the rate constant for the displacement of the first chloride, $k_2^{296} = 6.9 \pm 0.5$ M^{-1}s^{-1}, was more than 133 times slower than for the reaction with TU, which further supports the I$_a$ nature of the substitution mechanism.

Introduction

Studies on the coordination chemistry of copper(II) complexes with chelates incorporating pyridine and amine donors have been of significant interest in recent years. This is partly because of their relevance to histidine coordinated copper proteins such as blue copper proteins, hemocyanin, tyrosinase and cytochrome *c* oxidase.[1] Most of the functional and structural models for metalloproteins have been prepared by varying the substituents of the ligands in order to match the spectral properties of the metalloproteins.[2] In continuation of our earlier work in the area of copper(II) chemistry,[3] we describe here the synthesis and crystal structure of the $[Cu^{II}(pytBuN_3)Cl_2]$ complex, where py*t*BuN$_3$ = 2,6-bis(3,5-di-*tert*-butylphenyliminomethyl)pyridine. The strategies behind the selection of this chelate are: (i) it will force monomeric trigonal bipyramidal or square-pyramidal stereochemistry on copper(II), (ii) the donor properties of the selected *N*,*N*,*N*-chelate are comparable to that of 2,2′,2′′-terpyridine (**1**), the most widely studied chelate of this class of ligand, which has the trimethine structural unit and it is well established that it normally behaves as planar, tridentate ligand towards various kinetically labile metal ions such as Cu^{II}, Zn^{II} and Cd^{II} halides, and (iii) the incorporation of two bulky *tert*-butyl moieties on the chelate that will cause steric crowding on copper(II) and may help to induce unusual coordination geometries and hence interesting mechanistic and redox properties (Figure 1).[4]

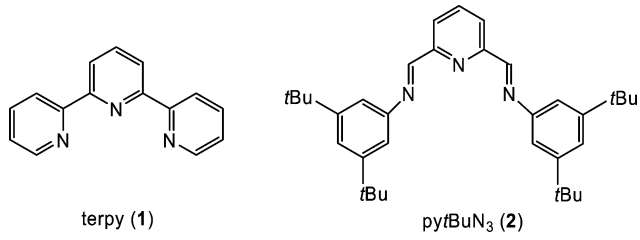

terpy (**1**) py*t*BuN$_3$ (**2**)

Figure 1. Schematic structure and abbreviations for the ligands.

We found that the synthesized $[Cu^{II}(pytBuN_3)Cl_2]$ complex has a distorted trigonal-bipyramidal structure. The present study also focuses on the mechanism of chloride substitution by thiourea (TU) and its derivative *N*,*N*,*N*′,*N*′-tetramethylthiourea (TMTU) as entering nucleophiles. As far as we know only a limited number of studies on the ligand substitution mechanism of five-coordinate copper(II) complexes have been reported.[3,4a,4b,5] Thiourea and *N*,*N*,*N*′,*N*′-tetramethylthiourea were selected as entering nucleophiles because of their high nucleophilicity that will prevent the back reaction with chloride. Furthermore, they were selected as a neutral entering ligand such that the overall reaction is accompanied by charge creation, and the for-

[a] Inorganic Chemistry, Department of Chemistry and Pharmacy, University of Erlangen-Nürnberg, Egerlandstr. 1, 91058 Erlangen, Germany

mation of the transition state may involve changes in dipole moment which will affect the activation parameters, especially the entropy and volume of activation. The selected $[Cu^{II}(pytBuN_3)Cl_2]$ complex contains bis-imine and pyridine in the back-bone of the ligand and is expected to be a strong π-acceptor ligand that will increase the electrophilicity of the metal centre.[6] We report here a detailed mechanistic study of the ligand-substitution reactions in methanol as a function of the entering nucleophile concentration, temperature and pressure.

Results and Discussion

Synthesis and Structure of $[Cu^{II}(pytBuN_3)Cl_2]$ Complex (3)

The ligand **2** was prepared in high yield from the condensation of two equivalents of 3,5-di-*tert*-butylaniline with one equivalent of pyridine-2,6-dicarbaldehyde (Scheme 1). The ligand was characterized by elemental analyses, and ^1H and ^{13}C NMR spectra confirmed its identity. Complex **3** was synthesized in good yield by treating $CuCl_2$ with **2** in methanol at room temperature. Complex **3** was characterized by elemental analyses and IR spectroscopy. The elemental analyses confirmed that the isolated complex was in accord with the formula $[Cu^{II}(pytBuN_3)Cl_2]$. The IR spectrum of ligand **2** shows that the C=N stretching frequency appears at 1626 cm^{-1}. In complex **3**, the C=N stretching shifts toward lower frequency at 1612 cm^{-1} and was greatly reduced in intensity, which points to the interaction between the imino nitrogens and the copper ion. In addition, the molecular and crystal structure of complex **3** was determined by a single-crystal X-ray diffraction study. A thermal ellipsoid plot of the molecular structure of complex **3** including the atom-numbering scheme is shown in Figure 2.

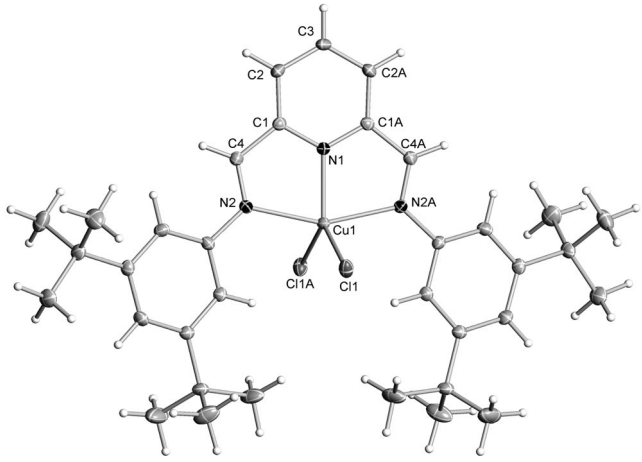

Figure 2. Thermal ellipsoid plot of the molecular structure of $[Cu^{II}(pytBuN_3)Cl_2]$ (**3**) showing the atom numbering scheme (50% probability level).

Relevant crystallographic data are given in Table 3, whereas selected bond lengths and bond angles are collected in Table 1. Complex **3** crystallizes in the monoclinic space group *C*2/*c*. The complex molecule is situated on a crystallographic twofold rotation axis running along the atoms Cu1, N1 and C3 (Wyckoff position 4*e*), thus exhibiting molecular C_2 symmetry. The molecular structure of the complex molecule involves a five-coordinate $[Cu^{II}(pytBuN_3)Cl_2]$ chromophore constituted by two imine (N2, N2A) and one pyridine (N1) nitrogen of the tridentate ligand and two chloride ions. The Cl1–Cu1–Cl1A angle is 119.22(2)° and due to the twofold symmetry the two N1–Cu–Cl angles are identical and amount to 120.39(2)°. In addition, in **3** the two imino C=N bonds have distinctive double-bond character, with C4=N2 distances of 1.287(2) Å. The Cu–N distances are shorter than the values reported in the literature for closely related complexes,[7] in-

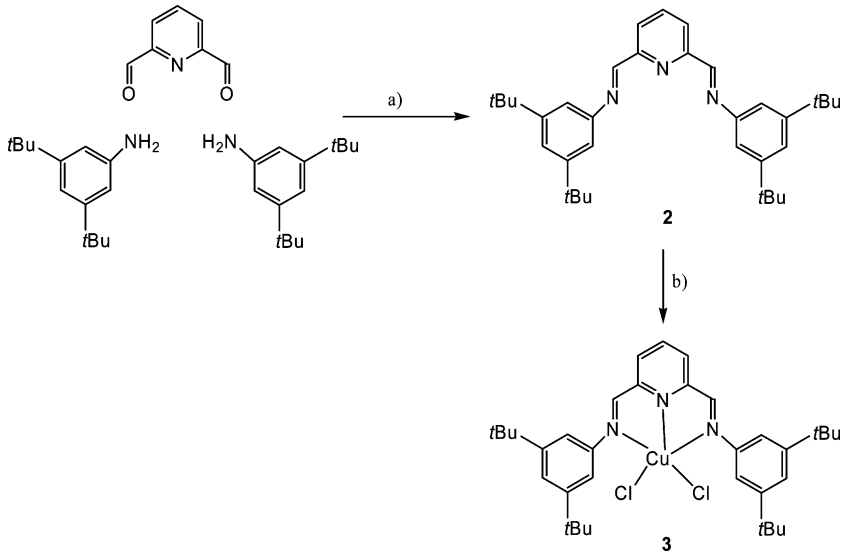

Scheme 1. Synthesis of the new $pytBuN_3$ ligand (**2**) and its copper(II) complex (**3**). a) MeOH, 23 °C, 6 h; b) $CuCl_2$, MeOH, 23 °C, 5 h.

dicating that the ligand is more tightly bound to the metal centre. The two phenyl rings are almost in the same plane of the CuN_3 backbone as in this arrangement the steric pressure between the bulky *tert*-butyl substituents and the chloride ions is reduced. The question arises as to whether the coordination polyhedron around the copper centre can be described as a square-pyramid or a trigonal bipyramid. Further information can be obtained by determining the structural index τ,[8] which represents the relative amount of trigonality [square pyramid, $\tau = 0$; trigonal bipyramid, $\tau = 1$; $\tau = (\beta - \alpha)/60$; where α and β being the two largest angles around the central atom]. The obtained value of 0.60 for the structural index τ reveals that the coordination geometry around copper(II) is best described as distorted trigonal-bipyramidal with an axis defined by the nitrogens N2 and N2A, and this axis is slightly bent towards the N1 atom resulting in an N2–Cu1–N2A angle of 156.26(7)°. The crystal packing of **3** is characterized by the formation of corrugated sheets perpendicular to the crystallographic *ac* plane. Between these sheets weak intermolecular C–H···Cl interactions with (C–)H···Cl distances in the range of 2.71–2.84 Å (Figure 3) are observed.

Table 1. Selected bond lengths [Å] and angles [°] for [Cu(py*t*BuN_3)Cl_2] (**3**).

Bond lengths [Å]		Bond angles [°]	
Cu(1)–N(1)	1.954(2)	N(2)–Cu(1)–N(1)	78.13(3)
Cu(1)–N(2)	2.123(2)	N(2A)–Cu(1)–N(1)	78.13(3)
Cu(1)–N(2A)	2.123(2)	N(2)–Cu(1)–N(2A)	156.26(7)
Cu(1)–Cl(1)	2.3049(4)	N(1)–Cu(1)–Cl(1)	120.39(2)
Cu(1)–Cl(1A)	2.3049(4)	N(1)–Cu(1)–Cl(1A)	120.39(2)
C(4)–N(2)	1.287(2)	N(2)–Cu(1)–Cl(1)	94.22(4)
C(4A)–N(2A)	1.287(2)	N(2)–Cu(1)–Cl(1A)	97.73(3)
		N(2A)–Cu(1)–Cl(1)	97.73(3)
		N(2A)–Cu(1)–Cl(1A)	94.22(4)
		Cl(1)–Cu(1)–Cl(1A)	119.22(2)

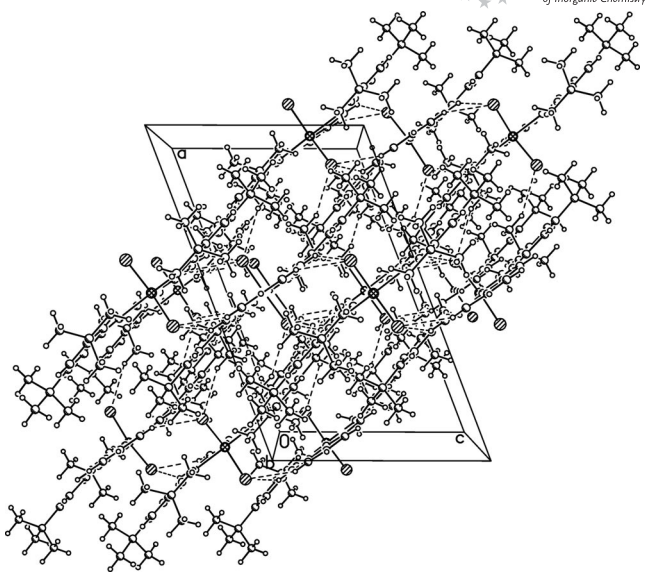

Figure 3. Formation of corrugated sheets perpendicular to the crystallographic ***ac*** plane in the crystal packing of complex **3** (weak intermolecular C–H···Cl interactions are indicated by dotted lines).

Electrochemical Studies on Complex 3

The electrochemical behaviour of complex **3** was studied to provide more information on the nature of the complex in solution. Cyclic voltammograms were recorded in MeOH solution vs. Ag/Ag^+ reference electrode. Complex **3** exhibits a one-electron reduction at 0.443 V and the corresponding oxidation occurs at 0.527 V, which can be assigned to the [Cu^{II}(py*t*BuN_3)Cl_2]$^{0/+}$ species. The complex [Cu^{II}(py*t*BuN_3)Cl_2] that undergoes reduction is completely regenerated following electrochemical oxidation (the ratio of the peak currents *i*pa/*i*pc is about 1.0), suggesting a chemically reversible Cu^{II}/Cu^{I} one-electron transfer process. However, the value of the limiting peak-to-peak separation (ΔE_p, 84 mV), which lies within the normal values for a reversible one-

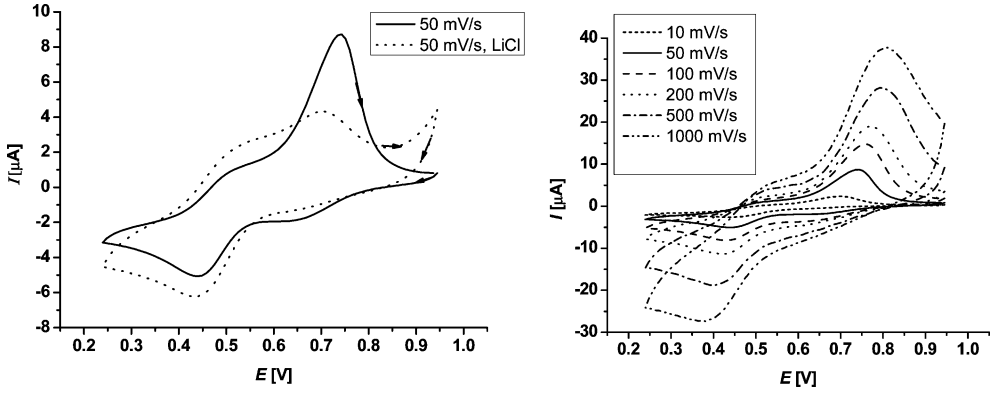

Figure 4. left) Cyclic voltammograms of [Cu^{II}(py*t*BuN_3)Cl_2] (– before and - - - after addition of 0.1 M LiCL); right) Cyclic voltammograms of [Cu^{II}(py*t*BuN_3)Cl_2] as a function of scan rate. Measurements were performed on a Pt working electrode vs. a non-aqueous Ag/Ag^+ reference electrode; add 544 mV [300 mV, Ag/Ag^+ to SCE; +244 mV, SCE to SHE] to convert to standard hydrogen electrode (SHE); Fc/Fc^+ couple in CH_3CN, $E_{1/2}$, 0.414 V (CV); (supporting electrolyte 10^{-3} M, 10^{-1} NBu_4PF_6, scan rate = 50 mV/s, potentials given in V, complex concentration, 0.2 mM).

electron redox process, suggests that the heterogeneous electron-transfer process in these complexes is easily reversible[9] (ΔE_p, 60 mV for a reversible one-electron redox process) and not accompanied by stereochemical reorganization.[10] An additional one-electron reduction occurs at 0.763 V and the corresponding oxidation at 0.652 V. The *i*pa/*i*pc value is far from unity, with a relatively higher ΔE_p values (111 mV), suggesting that the complex undergoes structural reorganization on electron transfer. This peak may arises from the oxidation of a four-coordinate Cu^I species obtained by loosing one chloride ion. Thus, when the scan rate is increased from 50 to 1000 mV (Figure 4) the additional peak grows in height, suggesting that at higher scan rates the Cu^I species is preferentially formed immediately on reducing the trigonal-bipyramidal $[Cu^{II}(py\textit{t}BuN_3)Cl_2]$ species. On addition of Cl^- ions (LiCl), the height of the additional peak decreases accompanied by an increase in the first peak, illustrating that the four-coordinate Cu^I species combines with the Cl^- ion to form a pentacoordinate Cu^I species, which decreases its concentration. Thus, the redox behaviour of **3** corresponds to the redox of two related species: four-coordinate $[Cu^{II}(py\textit{t}BuN_3)Cl]^{+/2+}$ species, reduced at more positive $E_{1/2}$ value, and the five-coordinate $[Cu^{II}(py\textit{t}BuN_3)Cl_2]^{0/+}$ species, reduced at less positive $E_{1/2}$ value (Scheme 2). Similar schemes have been demonstrated to exist for $Cu^{II/I}$ complex systems of the tridentate bis(benzimidazole-2′-yl) ligand.[11]

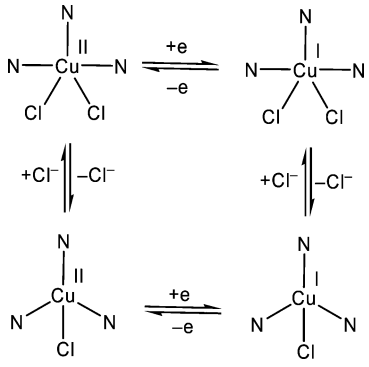

Scheme 2. Square scheme that accounts for the observed cVs.

Kinetic Studies

The reactions of $[Cu^{II}(py\textit{t}BuN_3)Cl_2]$ (**3**) with thiourea and *N*,*N*,*N*′,*N*′-tetramethylthiourea can be monitored kinetically in the range of ca. 360–440 nm. Solutions were prepared by dissolving known amounts of the chloro complex in methanol in the presence of 0.002 M LiCl in order to prevent the spontaneous solvolysis reactions. The ligand-substitution reactions were studied as a function of TU and TMTU concentration, temperature and pressure in methanol. An example of the UV/Vis spectral changes and a representative kinetic trace are shown in Figure 5.

Rate constants for the reactions were determined by using total TU and TMTU concentrations in the range of 0.001–0.125 M, i.e. always at least in 10-fold excess over the

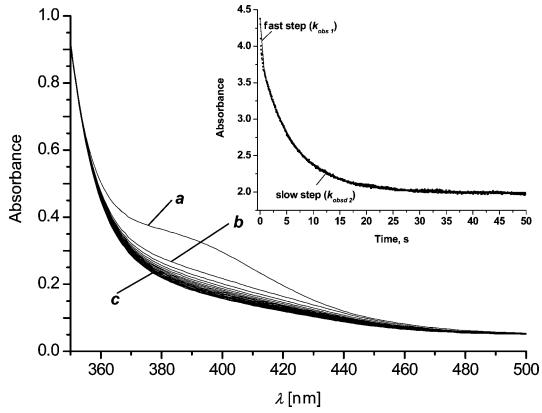

Figure 5. UV/Vis spectral changes recorded for the reaction of complex **3** (1×10^{-4} M) with thiourea (0.125 M) in methanol at 296 K: (a) spectrum before the reaction; (b) spectrum obtained several milliseconds after mixing of the reactants in the stopped-flow apparatus; (c) spectrum obtained after 50 s.

Cu^{II} complex. Throughout the nucleophile concentration range it was possible to fit the absorbance/time traces to a two-exponential function by using Equation (1). However, in the case of TMTU the second reaction was too slow to obtain accurate rate constants and we only analysed the first reaction step in more detail (see Figure 6).

$$A = a_1[\exp(-k_{obsd.1}t)] + a_2[\exp(-k_{obsd.2}t)] + A_0 \quad (1)$$

This means that the overall reaction is biphasic, as shown in Figure 6 for typical kinetic traces. An initial fast reaction (rate constant $k_{obsd.1}$) is followed by a much slower one (rate constant $k_{obsd.2}$). Rate constant $k_{obsd.1}$ increases linearly with TU concentration (Figure 7), which leads to second-order rate constant $k_1 = 918 \pm 30\ M^{-1}s^{-1}$. Rate constant $k_{obsd.2}$ also depends linearly on the TU concentration and the second-order rate constant was found to be $k_2 = 1.62 \pm 0.06\ M^{-1}s^{-1}$ (Figure 7). The rate constants demonstrate that the second substitution is slowed down almost 570 times due to the displacement of one chloride ligand by thiourea.

A similar concentration dependence was found for the first reaction step with TMTU as shown in Figure 8, from which it follows that $k_1 = 6.9 \pm 0.5\ M^{-1}s^{-1}$ at 296 K. The second substitution step was not studied in more detail for TMTU as entering ligand as mentioned before. A comparison of k_1 with that found for TU as entering nucleophile indicates that the introduction of four methyl substituents slows down the reaction 133 times at 296 K.

The observed kinetic behaviour can be accounted in terms of two subsequent substitution reactions (2) and (3) in which the two chloride ligands are subsequently displaced by either TU or TMTU (Nu) characterized by the second-order rate constants k_1 and k_2, respectively.

$$[Cu^{II}(L)Cl_2] + Nu \rightarrow [Cu^{II}(L)(Cl)(Nu)] \qquad k_1 \quad (2)$$

$$[Cu^{II}(L)(Cl)(Nu)] + Nu \rightarrow [Cu^{II}(L)(Nu)_2] \qquad k_2 \quad (3)$$

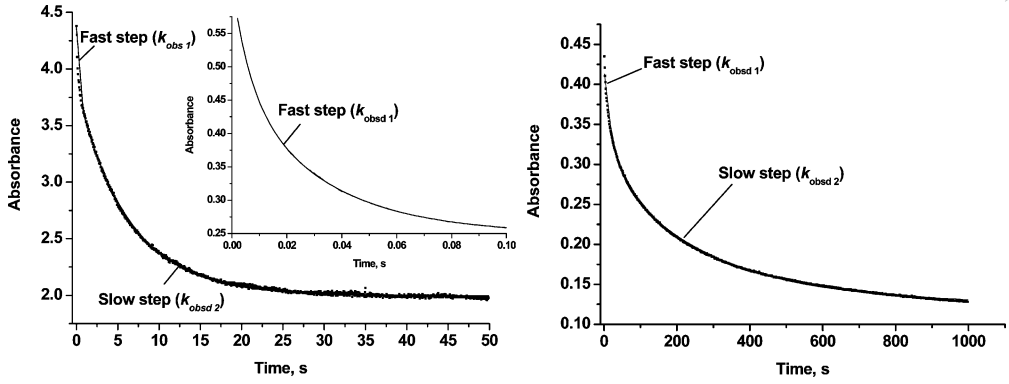

Figure 6. Absorbance-time traces at 394 nm for the reaction of complex **3** (1×10^{-4} M) with 0.125 M thiourea (left, inset is the fast reaction measured by stopped-flow instrument) and *N*,*N*,*N*′,*N*′-tetramethylthiourea (right) in methanol at 296 K (solid line obtained by fitting the data to Equation (1)).

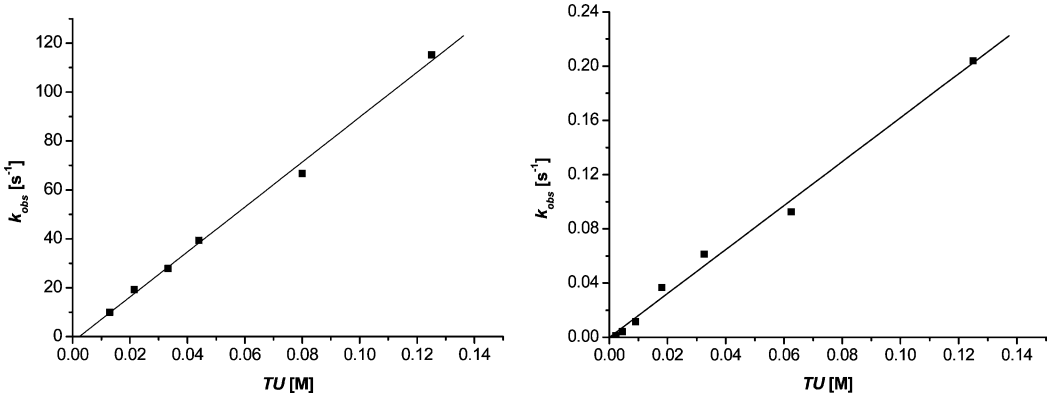

Figure 7. Plot of k_{obsd} vs. thiourea concentration for complex **3** in methanol at 296 K (left: first reaction step; right: second reaction step). Experimental conditions: [**3**] = 0.1 mM, 0.002 M LiCl, wavelength 394 nm.

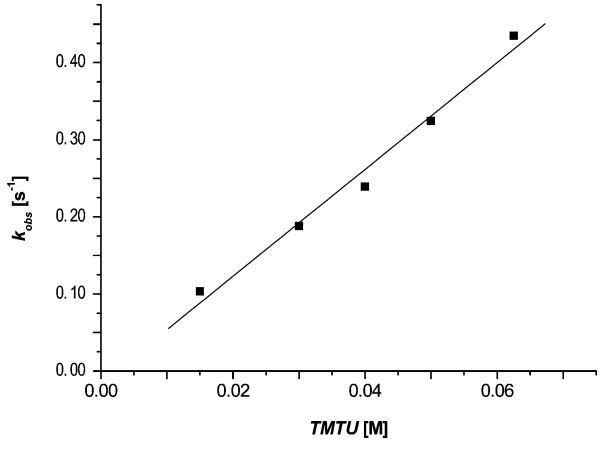

Figure 8. Plot of k_{obsd} vs. [TMTU] for the reaction with complex **3** in methanol at 296 K. Experimental conditions: [**3**] = 0.1 mM, 0.002 M LiCl, wavelength 394 nm.

It follows from this reaction Scheme that $k_{obsd.1}$ and $k_{obsd.2}$ should depend linearly on the entering nucleophile concentration in the absence of a back reaction as shown in Figures 7 and 8, such that $k_{obsd.1} = k_1$[Nu] and $k_{obsd.2} = k_2$[Nu].

The activation parameters ($\Delta H^{\neq}$, $\Delta S^{\neq}$ and $\Delta V^{\neq}$) were determined from the temperature and pressure dependence of k_1 and k_2 for both substitution reactions of complex **3** in methanol, and are summarized in Table 2. Representative plots that show typical temperature and pressure dependences are reported in Figures 9, 10, and 11, respectively.

Table 2. Summary of rate and activation parameters for the displacement of coordinated chloride on complex **3** by thiourea (TU) and *N*,*N*,*N*′,*N*′-tetramethylthiourea (TMTU) in methanol.

Activation parameters	TU		TMTU
	first reaction	second reaction	first reaction
k_2^{96} [M^{-1} s^{-1}]	918 ± 30	1.62 ±0.06	6.9 ± 0.5
$\Delta H^{\#}$ [kJ mol^{-1}]	42 ± 2	58 ± 2	52 ± 2
$\Delta S^{\#}$ [J K^{-1} mol^{-1}]	–46 ± 7	–47 ± 6	–58 ± 8
$\Delta V^{\#}$ [cm^3 mol^{-1}]	–6.5 ± 0.2	–5.3 ± 0.7	–

As seen from the summary of the rate constants in Table 2, the second substitution reaction with thiourea is much slower than the first one, which can be ascribed to steric hindrance on the Cu^{II} center in complex **3** caused by the displacement of chloride by thiourea. Furthermore, the values of k_1 for reaction (2) decrease significantly on going

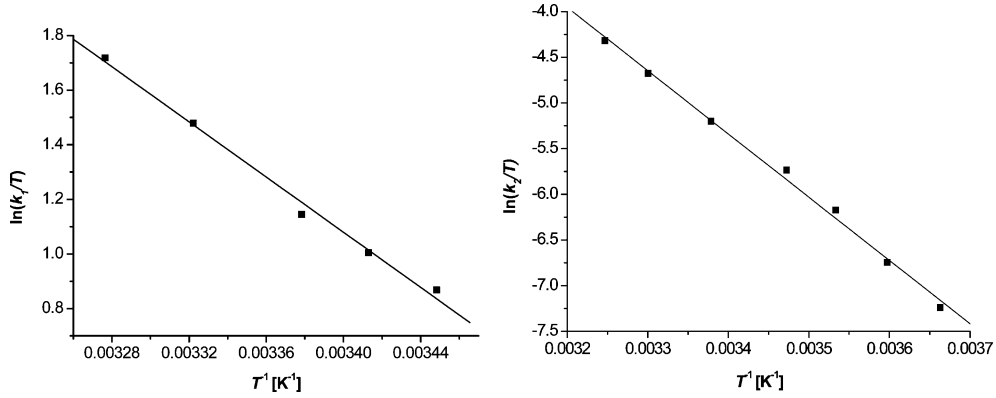

Figure 9. Temperature dependence of the reactions of complex **3** with thiourea in methanol (left, first reaction step, right: second reaction step). Experimental conditions: [**3**] = 0.1 mM, [TU] = 0.125 M, 0.002 M LiCl.

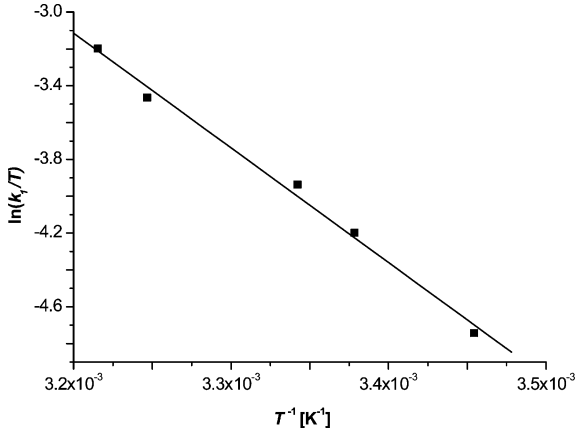

Figure 10. Temperature dependence of the first reaction of complex **3** with TMTU in methanol. Experimental conditions: [**3**] = 0.1 mM, [TMTU] = 0.125 M, 0.002 M LiCl.

from TU to TMTU as a result of the steric hindrance caused by the four methyl substituents. Both these trends suggest that ligand substitution on complex **3** follows an associatively activated mechanism that is controlled by bond formation between the entering nucleophile and the Cu^{II} center. Thus the transition state of the process is expected to have six-coordinate character on forming a bond between the five-coordinate Cu^{II} complex and the entering nucleophile. The activation parameters reported in Table 2 also support this suggestion. The values of $\Delta S^{\#}$ and $\Delta V^{\#}$ are all significantly negative and support the operation of an associative mechanism for both reactions (2) and (3). The magnitude of the activation volumes are such that it supports the operation of an associative interchange (I_a) mechanism rather than a limiting associative (A) mechanism.[12,13] Similar results were reported for water exchange and ligand-substitution reactions on the five-coordinate $[Cu(tren)H_2O]^{2+}$ and substituted tren complexes.[3c] In this case however, only one ligand can be replaced in comparison to two ligands on the studied complex **3**. For instance the water exchange reaction on $[Cu(tren)H_2O]^{2+}$ is three orders of magnitude slower than on fully aquated $[Cu(H_2O)_6]^{2+}$ and characterized by $\Delta S^{\#} = -34 \pm 5$ J K^{-1} mol^{-1} and $\Delta V^{\#} = -4.4 \pm 0.2$ cm^3 mol^{-1}, which is clearly in line with an associative interchange mechanism. Similarly, the reversible substitution reactions of $[Cu(tren)H_2O]^{2+}$ with pyridine and substituted pyridines are all characterized by negative $\Delta S^{\#}$ and $\Delta V^{\#}$ demonstrating that in all cases the transition states are more compact than either the reactant or product states.[3c,14] The magnitude of the activation volumes reported in Table 2 and those for the substitution reactions on $[Cu(tren)H_2O]^{2+}$ is in line with an I_a substitution mechanism for these trigonal bipyramidal complexes.

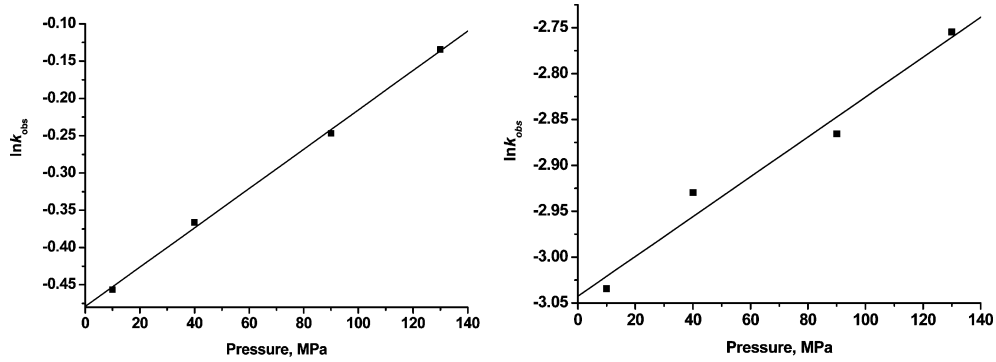

Figure 11. Pressure dependence of the reaction of complex **3** with thiourea in methanol (left: first reaction step, right: second reaction step). Experimental conditions: [**3**] = 0.1 mM, [TU] = 0.015 M, 296 K, 0.002 M LiCl.

Conclusions

A five-coordinate copper(II) complex with a sterically constrained py*t*BuN_3 chelate ligand [py*t*BuN_3 = 2,6-bis(3,5-di-*tert*-butylphenyliminomethyl)pyridine] has been synthesized and characterized by X-ray crystal structure determination. In the crystal structure of the complex the [Cu(py*t*BuN_3)Cl_2] chromophore possesses a distorted trigonal-bipyramidal coordination geometry in which the two imine nitrogen atoms occupy the two axial positions. The kinetics and mechanism of chloride substitution by thiourea (TU) and *N*,*N*,*N*′,*N*′-tetramethylthiourea (TMTU) were studied in detail as a function of entering nucleophile concentration, temperature and pressure in methanol as solvent. The kinetics showed that the substitution reaction of [Cu(py*t*BuN_3)Cl_2] is a biphasic process that involves the subsequent displacement of both chloride ligands. The substitution of the first chloride by TU is 570 times faster than the substitution of the second chloride. The activation parameters of both reactions support an associative interchange (I_a) substitution mechanism. When the substitution reaction was carried out with the sterically hindered nucleophile TMTU, the rate constant for the displacement of the first chloride was more than 133 times slower than for the reaction with TU, which further supports the I_a nature of the substitution mechanism.

Experimental Section

General: All chemicals used were of analytical reagent grade and of the highest purity commercially available. Copper(II) chloride dihydrate (Aldrich) was used without further purification. Pyridine-2,6-dicarbaldehyde was synthesized as described in the literature.[15]

Synthesis of 3,5-di-*tert*-Butylaniline: 3,5-Di-*tert*-butylaniline was prepared in a similar way as described in the literature.[16] At 45 °C, NaN_3 (1.84 g, 28.2 mmol) was added slowly during 1 h to a suspension of 3,5-di-*tert*-butylbenzoic acid (**1**) (6.92 g, 30 mmol) in a mixture of concentrated H_2SO_4 (20 mL) and $CHCl_3$ (20 mL). The mixture was further stirred for another 5 h at 45 °C. $CHCl_3$ was removed under vacuo and H_2O (100 mL) was added (***Caution!***) to the residue at 0 °C. The resultant solid was isolated by filtration, washed with H_2O (30 mL) to give 3,5-di-*tert*-butylanilinium sulfate as a colorless solid. This solid was resuspended in MeOH (20 mL), neutralized with KOH (10%) and the resulting solid was isolated by filtration, washed with H_2O (100 mL) and dried in vacuo. Yield 4.86 g (80%). ^{1}H NMR (269.6 MHz, CD_2Cl_2, 23 °C): δ = 1.28 (s, 18 H, 2 *t*Bu), 3.61 (br., 2 H, N*H*$_2$), 6.53 (d, 1 H, Ar-*H*), 6.81 (m, 1 H, Ar-*H*) ppm. IR (KBr): $\tilde{\nu}$ = 3380 (w, N–H). MS (FD$^+$, CH_2Cl_2): *m*/*z* = 205 [M]$^+$. $C_{14}H_{23}N$ (205.34): calcd. C 81.89, H 11.29, N 6.82; found C 82.79, H 11.97, N 6.31.

Synthesis of 2,6-Bis(3,5-di-*tert*-butylphenyliminomethyl)pyridine (2): Pyridine-2,6-dicarbaldehyde (0.135 g, 1.0 mmol) and 3,5-di-*tert*-butylaniline (0.410 g, 2.0 mmol) were stirred in methanol (25 mL) for 6 h in the course of which a yellow solid was formed. This solid was filtered off, washed with cold methanol and dried in vacuo to give **2**·CH_3OH in 96% yield. $C_{36}H_{51}N_3O$ (541.82): calcd. C 79.80, H 9.49, N 7.76; found C 79.76, H 9.00, N 7.98. ^{1}H NMR (400 MHz, $CDCl_3$, 23 °C): δ = 8.76 (s, 2 H, *H*C=N), 8.31 (d, *J* = 7.4 Hz, 2 H, $H_{\beta\ pyridine}$), 7.95 (t, *J* = 7.5 Hz, 1 H, $H_{\gamma\ pyridine}$), 7.37 (m, 2 H, $H_{arom.}$), 7.19 (m, 2 H, $H_{arom.}$), 1.37 {s, 36 H, [C(CH_3)$_3$]} ppm. ^{13}C NMR (100 MHz, $CDCl_3$, 23 °C): δ = 159.2 (*C*H=N), 154.8, 151.91, 150.08, 137.32, 123.09, 121.22, 115.62, ($C_{arom.}$), 35.05 [*C*(CH$_3$)$_3$], 31.48 [C(*C*H$_3$)$_3$] ppm. IR (KBr): $\tilde{\nu}$, cm^{-1} 3062 (s, C-$H_{arom.}$), 2962 (s, C-H_{aliph}), 1626 (m, C=N), 1595, 1585, 1523 (s, C=$C_{arom.}$). MS (FD$^+$, $CHCl_3$): *m*/*z* = 510 [M]$^+$.

Synthesis of the Complex [Cu(*t*BupyN$_3$)Cl$_2$] (3): $CuCl_2$ (0.403 g, 0.3 mmol) was added to a suspension of 2,6-bis(3,5-di-*tert*-butylphenyliminomethyl)pyridine (**2**) (1.53 g, 0.3 mmol) in methanol and the mixture was stirred for 5 h. The resultant orange-brown product was filtered off, washed with cold methanol (5 mL) and dried in vacuo to give **3** in 75% yield. $C_{35}H_{47}Cl_2CuN_3$ (644,22): calcd. for C 65.25, H 7.35, N 6.52; found C 64.98, H 7.42, N 6.65. IR (KBr): $\tilde{\nu}$, cm^{-1} 3087 (s, C-$H_{arom.}$), 2958 (s, C-H_{aliph}), 1612 (m, C=N). MS (FD$^+$, CH_3OH): *m*/*z* = 610 [M – Cl]$^+$.

Instrumentation and Measurements: Spectra were recorded with the following instruments: IR (KBr discs, solvent bands were compensated): Mattson Infinity instrument (60 AR) at 4 cm^{-1} resolution in the 400–4000 cm^{-1} range; NMR: Jeol-JNM-GX 270, EX 270, and Lambda LA 400 with the protio-solvent signal used as an internal reference. Mass spectra: Jeol MSTATION 700 spectrometer; elemental analyses: Carlo–Erba EA 1106 or 1108 analyzer. Cyclovoltammetric (CV) measurements were performed in a one-compartement three-electrode cell using a gold working electrode (Metrohm) with a geometrical surface of 0.7 cm^2 connected to a silver wire pseudo-reference electrode and a platinum wire serving as counter electrode (Metrohm). Measurements were recorded with an Autolab PGSTAT 30 unit at room temperature. The working electrode surface was cleaned using 0.05 μm alumina sonicated and washed with water every time before use. The working volume of 10 mL was deaerated by passing a stream of high purity N_2 through the solution for 15 min prior to the measurements and then maintaining an inert atmosphere of N_2 over the solution during the measurements. All CVs. were recorded for the reaction mixture with a sweep rate of 50 mV s^{-1} at 25 °C. Potentials were measured in 0.1 M TBAP electrolyte solution and are reported vs. an Ag/AgCl electrode. Kinetic investigations of the substitution of the dichloro complex by thiourea or tetramethylthiourea were performed either in tandem cuvettes with a path length of 0.88 cm, thermally equilibrated at 23 ± 0.1 °C before mixing, using a Varian Cary 1G spectrophotometer, or on an Applied Photophysics SX 18MV stopped-flow instrument (also thermostatted at 23.0 ± 0.1 °C) with an optical pathlength of 1 cm at 394 nm. For experiments at elevated pressure (1–130 MPa), a laboratory-made high-pressure stopped-flow instrument was used.[17] The temperature of the instruments was controlled with an accuracy of ±0.1 °C. Thiourea and *N*,*N*,*N*′,*N*′-tetramethylthiourea were selected as entering nucleophile since their high nucleophilicity prevents the back reaction with chloride. LiCl solutions (0.002 M) were used to avoid spontaneous solvolysis of the chloro complexes. The ligand-substitution reactions were studied under pseudo-first-order conditions by using at least a ten-fold excess of thiourea or tetramethylthiourea. All listed rate constants represent an average value of at least three kinetic runs under each experimental condition.

Data Collection and Structure Refinement: Orange needle-shaped single crystals of **3** were grown from a saturated CH_3OH solution at room temperature in the course of three days. A suitable single crystal was mounted on top of a glass capillary using protective perfluoropolyalkyl ether oil. Intensity data were collected on a Bruker–Nonius Kappa CCD diffractometer using Mo-K_α radiation (λ = 0.71073 Å, graphite monochromator). An empirical absorption correction based on multiple scans using SADABS[18] was per-

formed. The structure was solved by direct methods and refined on F^2 using full-matrix least-squares procedures (SHELXTL NT 6.12).[19] Hydrogen atoms were geometrically positioned and allowed to ride on the corresponding carrier atoms with their isotropic displacement parameter fixed at 1.2 or 1.5 times U_{eq} of the proceeding C atom. Table 3 summarizes selected crystallographic data, data collection and structure refinement details.

Table 3. Crystallographic data and structure refinement for complex [Cu(py*t*BuN$_3$)Cl$_2$] (**3**).

Empirical formula	$C_{35}H_{47}Cl_2CuN_3$
Formula weight	644.20
Crystal size [mm]	$0.38 \times 0.06 \times 0.05$
Crystal system	monoclinic
Space group	*C*2/*c*
a [Å]	18.050(2)
b [Å]	18.172(2)
c [Å]	11.0018(6)
α [°]	90
β [°]	110.896(5)
γ [°]	90
V [Å^3]	3371.3(4)
Z	4
μ [mm^{-1}]	0.834
$D_{calcd.}$ [g cm^{-3}]	1.269
F(000)	1364
Reflections collected	54802
Reflections independent	4356
Reflections observed [$I > 2\sigma(I)$]	3622
Data/restraints/parameters	4356/0/193
Goodness-of-fit on F^2	1.047
Final *R* indices [$I > 2\sigma(I)$]	$R_1 = 0.0306$, $wR_2 = 0.0662$
R indices (all data)	$R_1 = 0.0440$, $wR_2 = 0.0712$
$\Delta\rho_{max/min}$	0.438/–0.396

CCDC-724398 contains the supplementary crystallographic data for complex **3**. These data can be obtained free of charge from the Cambridge Crystallographic Data Centre via www.ccdc.cam.ac.uk/data_request/cif.

Acknowledgments

The authors gratefully acknowledge financial support from the Deutsche Forschungsgemeinschaft (DFG) and the Ägyptische Studienmission.

[1] a) J. J. da Silva, R. J. P. Williams, *The Biological Chemistry of the Elements – The Inorganic Chemistry of Life*, Clarendon, Oxford, England, **1991**; b) H. Sigel (Ed.), *Perspectives in Coordination Chemistry*, Verlag Helvetica Chimica Acta Basel, **1992**.

[2] a) R. T. Jonas, T. D. P. Stack, *Inorg. Chem.* **1998**, *37*, 6615; b) N. Wei, N. N. Murthy, Q. Chen, J. Zubieta, K. D. Karlin, *Inorg. Chem.* **1994**, *33*, 1953; c) K. D. Karlin, R. W. Cruse, Y. Gultneh, A. Farooq, J. C. Hayes, J. Zubieta, *J. Am. Chem. Soc.* **1987**, *109*, 2668; d) N. Kitajima, T. Koda, S. Hashimoto, T. Kitagawa, Y. Moro-oka, *J. Am. Chem. Soc.* **1991**, *113*, 5664.

[3] a) F. Thaler, C. D. Hubbard, F. W. Heinemann, R. van Eldik, S. Schindler, I. Fabian, A. M. Dittler-Klingemann, F. E. Hahn, C. Orvig, *Inorg. Chem.* **1998**, *37*, 4022; b) M. Becker, S. Schindler, R. van Eldik, *Inorg. Chem.* **1994**, *33*, 5370; c) D. Hugh Powell, A. E. Merbach, I. Fabian, S. Schindler, R. van Eldik, *Inorg. Chem.* **1994**, *33*, 4468; d) A. Company, J.-E. Jee, X. Ribas, J. M. Lopez-Valbuena, L. Gmez, M. Corbella, A. Llobet, J. Maha, J. Benet-Buchholz, M. Costas, R. van Eldik, *Inorg. Chem.* **2007**, *46*, 9098; e) M. M. Ibrahim, S. Y. Shaban, *Inorg. Chim. Acta* **2009**, *362*, 1471.

[4] a) D. B. Rorabacher, *Chem. Rev.* **2004**, *104*, 651–698; b) D. E. Fenton, *Chem. Soc. Rev.* **1999**, *28*, 159; c) N. Kitajima, *Adv. Inorg. Chem.* **1992**, *39*, 1; d) E. T. Adman, *Adv. Protein Chem.* **1991**, *42*, 145.

[5] a) G. R. Cayley, l. D. Kelly, P. F. Knowles, K. D. S. Yadav, *J. Chem. Soc., Dalton Trans.* **1981**, 2370; b) G. R. Cayley, D. Gross, P. F. Knowles, *J. Chem. Soc., Chem. Commun.* **1976**, 837; c) D. P. Rabeln, H. W. Dodgen, J. P. Hunt, *J. Chem. Soc.* **1972**, *94*, 1771.

[6] A. Hofmann, D. Jaganyi, O. Q. Munro, G. Liehr, R. van Eldik, *Inorg. Chem.* **2003**, *42*, 1688.

[7] a) R. Balamurugan, M. Palaniandavar, M. A. Halcrow, *Polyhedron* **2006**, *25*, 1077; b) A. W. Addison, T. Nageswara Rao, E. Sinn, *Inorg. Chem.* **1984**, *23*, 1957; c) J. M. Holland, X. Liu, J. P. Zhao, F. E. Mabbs, C. A. Kilner, M. T. Pett, M. A. Halcrow, *J. Chem. Soc., Dalton Trans.* **2000**, 3316; d) R. J. Restivo, G. Ferguson, *J. Chem. Soc., Dalton Trans.* **1976**, 518; e) A. J. Blake, A. J. Lavery, M. Schroder, *Acta Crystallogr., Sect. C* **1996**, *52*, 37; f) M. Trivedi, D. S. Pandey, Q. Xu, *Inorg. Chim. Acta* **2007**, *360*, 2492.

[8] a) A. W. Addison, T. N. Rao, J. Reedijk, J. Rijn, G. C. Verschoor, *J. Chem. Soc., Dalton Trans.* **1984**, 1349; b) S. Uhlenbrock, R. Wagner, B. Krebs, *J. Chem. Soc., Dalton Trans.* **1996**, 3731.

[9] E. R. Brown, R. F. Large, in *Techniques of Chemistry: Physical Methods of Chemistry* (Eds.: A. Weissberger, B. Rossiter); Wiley: New York, **1971**; Vol. 1, Part IIA, p. 475.

[10] K. D. Karlin, P. L. Dahlstrom, J. R. Hyde, J. Zubieta, *J. Chem. Soc., Chem. Commun.* **1980**, 906.

[11] a) Sanaullah, K. Kano, R. S. Glass, G. S. Wilson, *J. Am. Chem. Soc.* **1993**, *115*, 592; b) S. Flanagan, J. Dong, K. Haller, S. Wang, W. R. Scheidt, R. A. Scott, T. R. Webb, D. M. Stanbury, L. J. Wilson, *J. Am. Chem. Soc.* **1997**, *119*, 8857; c) Y. Kuchiyama, N. Kobayashi, H. D. Takagi, *Inorg. Chim. Acta* **1998**, *277*, 31; d) M. J. Martin, J. F. Endicott, L. A. Ochrymowycz, D. B. Rorabacher, *Inorg. Chem.* **1987**, *26*, 3012; e) N. E. Meagher, K. L. Juntunen, C. A. Salhi, L. A. Ochrymowycz, D. B. Rorabacher, *J. Am. Chem. Soc.* **1992**, *114*, 10411; f) P. V. Robandt, R. R. Schroeder, D. B. Rorabacher, *Inorg. Chem.* **1993**, *32*, 3957; g) N. M. Villeneuve, R. R. Schroeder, L. A. Ochrymowycz, D. B. Rorabacher, *Inorg. Chem.* **1997**, *36*, 4475; h) R. Balamurugan, M. Palaniandavar, *Inorg. Chem.* **2001**, *40*, 2246.

[12] a) R. van Eldik, *Coord. Chem. Rev.* **2007**, *251*, 1649; b) J. Burgess, *Metal Ions in Solution*, Ellis Horwood, Chichester, **1978**; c) C. H. Langford, H. B. Gray, *Ligand Substitution Processes*, W. A. Benjamin, New York, Amsterdam, **1965**, p. 8.

[13] T. W. Swaddle, *Coord. Chem. Rev.* **1974**, *14*, 217.

[14] a) C. F. Weber, R. van Eldik, *Eur. J. Inorg. Chem.* **2005**, 4755; b) M. L. Tobe, J. Burgess, *Inorganic Reaction Mechanisms*, Addison Wesley Longman Limited, Essex, UK, **1999**, p. 10.

[15] N. W. Alcock, R. G. Kingston, P. Moore, C. Pierpoint, *J. Chem. Soc., Dalton Trans.* **1984**, 1937.

[16] S. Y. Shaban, M. M. Ibrahim, F. W. Heinemann, *Inorg. Chim. Acta* **2007**, *360*, 2929.

[17] R. van Eldik, W. Gaede, S. Wieland, J. Kraft, M. Spitzer, D. A. Palmer, *Rev. Sci. Instrum.* **1993**, *64*, 1355.

[18] *SADABS 2.10*, Bruker-AXS, Inc., Madison, WI, USA, **2002**.

[19] *SHELXTL NT* 6.12, Bruker-AXS, Inc., Madison, WI, USA, **2002**.

Received: April 1, 2009
Published Online: June 17, 2009

